Electronic Journal of Biotechnology 78 (2025) 35–45

Contents lists available at ScienceDirect

Electronic Journal of Biotechnology

journal homepage: www.elsevier.com/locate/ejbt

Research article

Transcriptomic and metabolomic profiling reveals key mechanisms of alkaline stress tolerance in rice ☆

Jiangxu Wang [a], Chuang Lang [a], Yang Ren [a], Junxiang Guo [b], Wendong Ma [b], Qing Liu [c], Lei Lei [d], Shichen Sun [d,*]

[a] Heilongjiang Academy of Agricultural Sciences, Harbin 150086, PR China
[b] Rice Research Institute of Heilongjiang Academy of Agricultural Sciences, Jiamusi 154000, PR China
[c] Suihua Branch of Heilongjiang Academy of Agricultural Sciences, Suihua 152000, PR China
[d] Heilongjiang Academy of Agricultural Sciences Institute of Cultivation, Harbin 150086, PR China

GRAPHICAL ABSTRACT

Transcriptomic and metabolomic profiling reveals key mechanisms of alkaline stress tolerance in rice

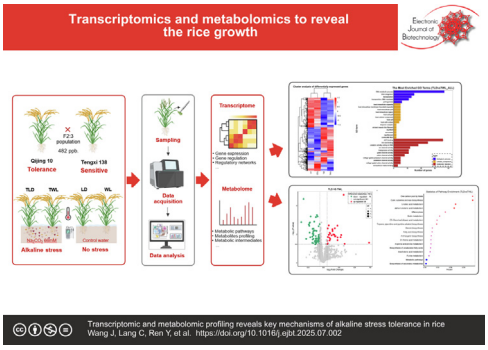

ARTICLE INFO

Article history:
Received 9 April 2025
Accepted 14 July 2025
Available online 25 August 2025

Keywords:
Alkaline stress tolerance
Antioxidant defense
Crop resilience
Membrane stability
Metabolomics
Oryza sativa

ABSTRACT

Background: Alkaline stress severely restricts rice growth and yield by disrupting ion balance, nutrient uptake, and oxidative metabolism. Clarifying the molecular mechanisms of tolerance is vital for breeding resilient varieties. This study explores transcriptional and metabolic adaptations in an alkali-tolerant (Qijing 10, LD) and sensitive (Tengxi 138, WL) rice variety under alkaline stress.
Results: Transcriptomic analysis revealed 1297 differentially expressed genes (DEGs) in the sensitive variety under alkaline stress (TWL), primarily enriched in pathways related to antioxidant enzyme synthesis (e.g., peroxidase genes), transmembrane ion transport, and membrane lipid stabilization pathways. In contrast, the tolerant variety (TLD) exhibited only 38 DEGs, suggesting transcriptional homeostasis achieved via suppression of stress-related gene overactivation. Metabolomic profiling demonstrated stable levels of key lipids (phosphatidic acid, galactolipids) and osmolytes (proline, betaine) in the tolerant variety under stress, whereas the sensitive variety accumulated lipid peroxidation products

☆ Audio abstract available in Supplementary material.
Peer review under responsibility of Pontificia Universidad Católica de Valparaíso.
* Corresponding author.
E-mail address: 13359870453@126.com (S. Sun).

https://doi.org/10.1016/j.ejbt.2025.07.002

Rice
Transcriptomics

(malondialdehyde, MDA) and displayed dysregulated carbohydrate metabolic dysregulation. Integrated multi-omics analysis indicated that the tolerant variety coordinated lipid metabolism gene modulation with antioxidant metabolite accumulation, establishing dual barriers for ROS scavenging and membrane protection. Conversely, transcriptional dysregulation in the sensitive variety led to metabolic collapse.
Conclusions: Alkaline tolerance in rice hinges on the synergistic modulation of stress-responsive genes and metabolic networks to preserve redox equilibrium and membrane function. The tolerant variety's capacity to stabilize transcriptional activity and metabolic flux underlies its resilience. These results elucidate key molecular and metabolic determinants of alkaline tolerance, offering strategic targets for breeding rice cultivars adapted to alkaline environments.
How to cite: Wang J, Lang C, Ren Y, et al. Transcriptomic and metabolomic profiling reveals key mechanisms of alkaline stress tolerance in rice. Electron J Biotechnol 2025;78. https://doi.org/10.1016/j.ejbt.2025.07.002.

1. Introduction

Soil alkalinity is a major environmental challenge affecting global crop production, particularly for rice (*Oryza sativa*), a staple food source for nearly half of the world's population [1,2]. While rice is well adapted to slightly acidic paddy soils, exposure to alkaline conditions can severely hinder its growth and productivity [3]. Alkaline stress disrupts ion homeostasis, reduces nutrient availability, and induces oxidative stress, collectively impairing key physiological processes such as root development, photosynthesis, and cellular metabolism [4,5]. Given the increasing prevalence of soil alkalinization due to unsustainable agricultural practices, climate change, and anthropogenic activities, developing rice varieties with enhanced tolerance to alkaline stress has become an urgent priority for global food security and sustainable crop management [6,7].

Over the past decade, advances in high-throughput omics technologies, particularly transcriptomics and metabolomics, have revolutionized our understanding of plant stress responses [7,8,9]. Transcriptomic analysis provides valuable insights into gene regulatory networks and stress-induced molecular pathways, including those related to ion transport, antioxidant defense, and hormonal signaling [10,11]. Meanwhile, metabolomics complements this by mapping the biochemical landscape of stress adaptation, identifying key metabolites involved in osmotic balance, reactive oxygen species (ROS) scavenging, and energy homeostasis [12,13]. By integrating these two approaches, researchers can construct a comprehensive framework linking transcriptional regulation to metabolic reprogramming, uncovering the intricate molecular mechanisms that underlie stress tolerance [14].

The ability to identify stress-responsive genes, metabolic pathways, and potential biomarkers is crucial for improving stress resilience in rice [15]. Recent studies have highlighted the role of lipid remodeling, amino acid metabolism, and secondary metabolite biosynthesis in conferring tolerance to abiotic stressors, including alkaline conditions [16,17,18]. However, the complex interplay between transcriptional and metabolic responses under alkaline stress remains insufficiently understood. A more in-depth exploration of these adaptive mechanisms will provide critical insights into how rice mitigates alkaline stress damage and maintains physiological stability.

In this study, we employ an integrative transcriptomic and metabolomic approach to systematically investigate the molecular basis of alkaline stress tolerance in rice. By analyzing gene expression patterns and metabolite fluctuations in a tolerant and a sensitive rice variety under alkaline conditions, we aim to elucidate key regulatory networks and metabolic pathways that contribute to stress adaptation. These findings will not only advance our fundamental understanding of plant-environment interactions but also provide a foundation for the development of genetically improved rice cultivars with enhanced resilience to alkaline soils. In the face of escalating climate change and soil degradation, leveraging omics-driven strategies to engineer stress-tolerant crops represents a vital step toward sustainable agriculture and global food security.

2. Materials and methods

2.1. Experimental materials

The experimental materials used in this study included the alkali-tolerant rice variety Qijing 10 (denoted as LD) and the alkali-sensitive rice variety Tengxi 138 (denoted as WL), alkali-treated group of Qijing 10 (TLD) and alkali-treated group of Tengxi 138 (TWL). These varieties were used as the parental lines to construct an F2:3 population, consisting of 482 individuals.

All plant materials were obtained from the Heilongjiang Academy of Agricultural Sciences. The parental lines and F2:3 population were cultivated at the experimental base of the academy during the 2022–2023 growing seasons. Seeds were pre-soaked and germinated in early April each year. Germinated seeds were sown in nursery beds between April 22 and April 24, followed by dry seedling raising, and subsequently transplanted into the field from May 20 to May 24. The experiment utilized a randomized block design with single-row plots, a row length of 2 m, row spacing of 30 cm, and hill spacing of 10 cm, with three replicates per treatment. To examine the response of different genotypes to alkaline stress, an alkaline treatment pool and a control pool were established, where all experimental materials were evenly divided and planted under the respective conditions.

2.2. Alkaline stress treatment

To simulate alkaline stress conditions, a $NaHCO_3$ solution with an electrical conductivity (EC) of 6 ds/m (~66 mM $NaHCO_3$) was used for irrigation, which corresponds to moderate-to-high alkaline conditions commonly observed in saline-alkali paddy soils of northeastern China. This concentration was selected based on previous studies that demonstrated its effectiveness in inducing alkali stress responses in rice. The pH of the treatment solution was maintained between 9.5 and 9.7 throughout the experimental period [19,20,21]. The control group received normal water irrigation. Alkaline stress treatment commenced at the tillering stage and continued until full maturity. To maintain a stable alkaline environment, the salt concentration in the treatment pool was monitored at 6:00, 12:00, and 20:00 daily. If fluctuations occurred due to rainfall or drought, appropriate adjustments were made through drainage or re-irrigation to restore the target concentration. Agro-

nomic management, including fertilization, pest control, and weed management, was performed in accordance with standard field cultivation practices to minimize external interference and ensure experimental accuracy [20,22].

2.3. Transcriptomic analysis

2.3.1. RNA isolation and qualification

The TRIzol extraction method (Invitrogen, CA, USA) was employed to isolate RNA, followed by treatment with RNase-free DNase I (Takara, Kusatsu, Japan) to ensure removal of DNA contaminants. RNA quality was confirmed through several steps: 1% agarose gels were used to assess degradation and contamination, a NanoDrop spectrophotometer (Thermo Scientific, DE, USA) measured RNA concentration and purity, and the Agilent 2100 Bioanalyzer (Agilent Technologies, CA, USA) evaluated RNA integrity [23].

2.3.2. Library preparation for transcriptome sequencing

Each sample was prepared using 1.5 μg of RNA and the NEBNext® Ultra™ RNA Library Prep Kit for Illumina® (NEB, USA). mRNA was purified, fragmented, and converted to cDNA, which was blunt-ended, adenylated, and ligated with NEBNext Adapters. cDNA fragments of 200–250 bp were selected and subjected to USER Enzyme treatment, followed by PCR amplification. The libraries were purified, quality-checked on the Agilent Bioanalyzer 2100, and sequenced on an Illumina Novaseq 6000 platform (Beijing Allwegene Technology Co., Beijing, China) to generate paired-end 150 bp reads [24,25].

2.3.3. Data analysis

We processed raw fastq reads through Perl scripts to obtain clean data by removing adapters, poly-N sequences, and low-quality reads, and calculated metrics like Q20, Q30, GC-content, and duplication level. Differential expression analysis used the DESeq package with a negative binomial model and adjusted p-values (Benjamini-Hochberg, $p < 0.05$). GO enrichment of differentially expressed genes (DEGs) was analyzed with GOseq to correct for gene length bias, and KEGG pathway enrichment was performed using KOBAS, identifying significant pathways in the DEGs [26,27,28].

2.4. Metabolomic analysis

2.4.1. Metabolites extraction

After removing the sample from the −80°C freezer, it was slowly thawed at 4°C. A specified volume of sample was combined with a chilled MeOH:CAN mixture (2:2:1, $v/v/v$) containing an internal standard and two steel beads. This mixture was ground at 60 Hz for 120 s and then sonicated for 10 min. Following incubation at −20°C for 1 h, the mixture was centrifuged at 13,000 rpm and 4°C for 15 min, and the supernatant was freeze-dried. For LC-MS/MS analysis, the dried sample was reconstituted in a CAN solution (1:1, v/v), vortexed for 30 s, sonicated for 10 min, and centrifuged again. The final supernatant was transferred to vials for injection. A pooled QC sample was prepared by mixing 10 μl from each sample.

2.4.2. UHPLC-MS-MS analysis

UHPLC analyses were performed using a Shimadzu LC-30 system paired with a TripleTOF 5600 + QTOF mass spectrometer (SCIEX) by Beijing Allwegene Technology Co., Ltd. Separation was conducted on an Acquity UHPLC system (SCIEX) using a Waters ACQUITY UPLC T3 column (100 mm × 2.1 mm, 1.7 μm, Waters), with the column oven set to 50°C. The flow rate was maintained at 0.3 ml/min. Solvent A (0.1% formic acid in water) and solvent B (0.1% formic acid in ACN) comprised the mobile phases. Gradient conditions were as follows: 0–0.5 min, 5% B; 0.5–2.5 min, ramped from 5% to 70% B; 2.5–7.5 min, 70–100% B; 7.5–9.0 min, 100% B; 9.0–9.5 min, 100–5% B; 9.5–12 min, 5% B. The high-resolution Triple TOF 5600 + mass spectrometer collected metabolic analytes in both positive and negative ionization modes. The instrument settings were as follows: Ion Source Gas1 and Gas2 at 50 psi, Curtain Gas at 35 psi, Source Temperature at 500°C, and an IonSpray Voltage Floating of 5500 V (positive) and −4500 V (negative). Declustering Potential (DP) was ± 80 V, with TOF MS scans covering an m/z range of 60–1200 Da and product ion scans spanning 25–1200 Da. Accumulation times were set to 0.25 s for TOF MS scans and 0.03 s for product ion scans. Secondary spectra were obtained using Information Dependent Acquisition (IDA) in High Sensitivity mode, with a Collision Energy (CE) of 30 V ± 15 [29,30]. Metabolite identification was conducted using ultra-high-performance liquid chromatography coupled with tandem mass spectrometry (UHPLC-MS/MS) in data-dependent acquisition (DDA) mode. Both primary MS and secondary MS/MS spectra were acquired for each sample. Accurate mass matching (mass error <10 ppm) and fragmentation pattern matching were performed against a comprehensive in-house spectral database established by the service provider, as well as publicly available metabolite databases including the Human Metabolome Database (HMDB), METLIN, and KEGG. According to the guidelines of the Metabolomics Standards Initiative (MSI), the confidence level of metabolite identification in this study corresponds primarily to Level 2, indicating putatively annotated compounds based on MS/MS spectral similarity to reference spectra in databases. For a subset of key metabolites, where both retention time and fragmentation ion patterns matched those of reference standards, the confidence level can be considered Level 1, representing confirmed identification. Metabolites lacking MS/MS spectral data or those with ambiguous matches were excluded from downstream biological interpretation.

2.4.3. Data analysis

After detecting X peaks, X metabolites were retained for analysis. Features detected in less than 50% of samples were removed, missing values were imputed with half the minimum, and internal standard normalization was applied. Features with RSD > 30% were excluded. The data were processed in MetaboAnalyst for PCA and OPLS-DA, with PCA showing data distribution and OPLS-DA enhancing group separation, calculating R^2 (variance explained) and Q^2 (predictive power). Model validation was conducted with a 200-time permutation test, and VIP scores identified significant variables. Metabolites with VIP > 1, $p < 0.05$, and Fold Change >1.5 or <0.67 were deemed significant, with pathway analysis performed via KEGG and MetaboAnalyst [31,32,33]. Metabolite Annotation Validation: Putative metabolites were filtered using the following criteria: (1) MS/MS spectral match score > 80% against authentic standards; (2) Presence in plant metabolite databases (PlantCyc, RiceCyc); (3) Biological relevance to abiotic stress. Compounds lacking plant endogenous evidence (e.g., triclosan) were excluded from functional analysis.

3. Results

3.1. Transcriptome analysis of differential gene expression under alkali stress

To investigate the transcriptional response to alkali stress, we performed RNA-seq analysis of an alkali-tolerant rice variety (Qijing 10) and an alkali-sensitive variety (Tengxi 138) under control and alkali stress conditions. Differential gene expression analysis revealed distinct transcriptional patterns between these groups,

with notable differences observed in the TLD vs. TWL and LD vs. TLD comparisons.

Volcano plot analysis (Fig. 1A) showed that in the TLD vs. TWL comparison, 1297 differentially expressed genes (DEGs) were identified, with 654 upregulated and 643 downregulated. This suggests substantial transcriptional divergence between the tolerant and sensitive varieties in response to alkali stress. In contrast, in the LD vs. TLD comparison, only 38 DEGs were detected (32 upregulated, 6 downregulated), indicating that Qijing 10 maintains a relatively stable transcriptional state under alkali stress. The hierarchical clustering heatmap (Fig. 1B) further supported this observation, showing clear separation between TWL and TLD, while LD and TLD exhibited greater transcriptomic similarity. Venn diagram analysis (Fig. 1C) identified 829 core DEGs shared across comparisons, which likely play key roles in the response to alkali stress. Notably, 68% of Qijing 10-specific DEGs exhibited consistently high expression under both control and stress conditions, suggesting a pre-adaptive transcriptional mechanism that contributes to its alkali tolerance.

3.2. GO and KEGG enrichment analysis of differentially expressed genes

To gain insights into the functional significance of the DEGs, Gene Ontology (GO) and Kyoto Encyclopedia of Genes and Gen-

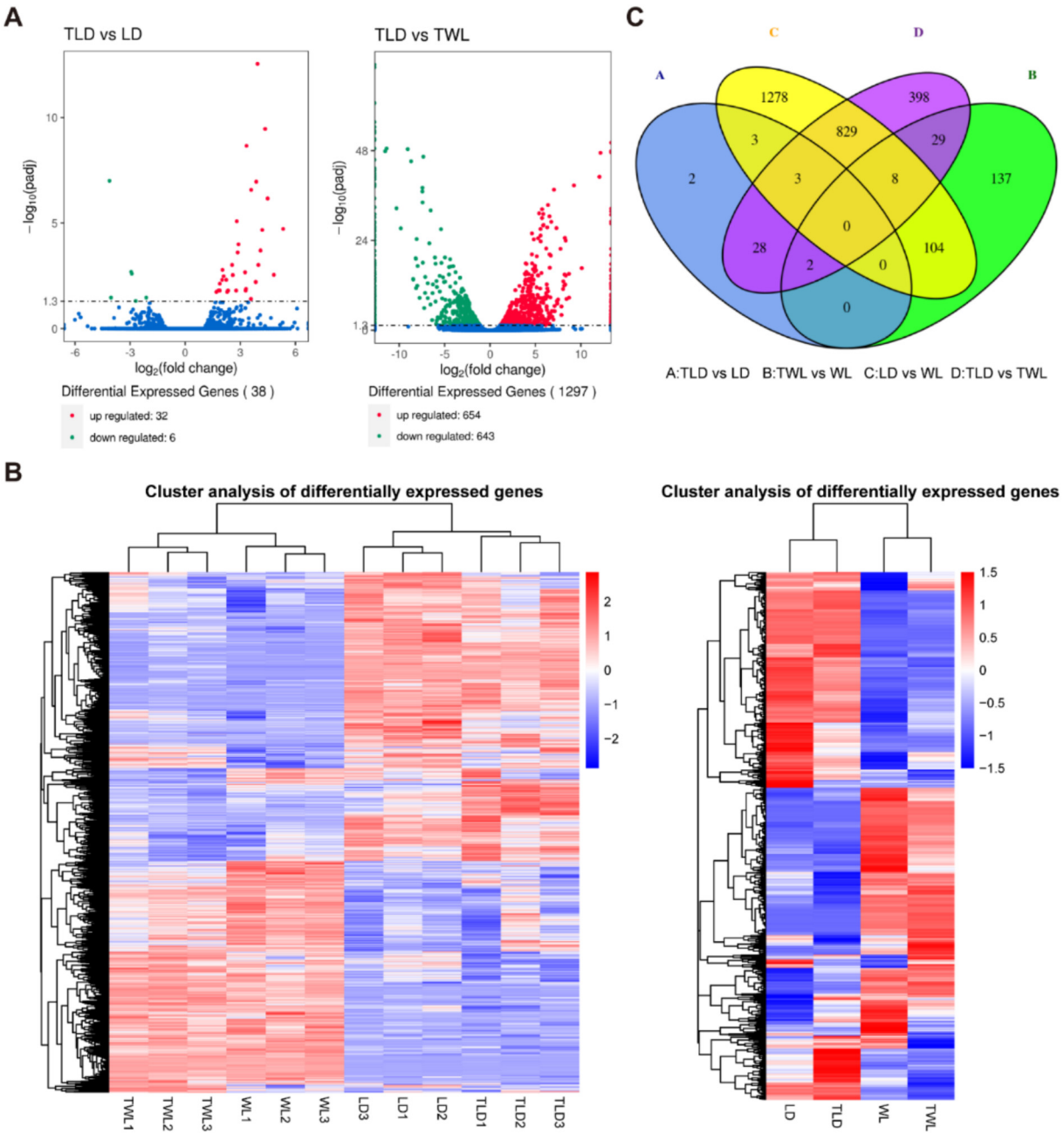

Fig. 1. Transcriptome profiling and clustering analysis of differentially expressed genes (DEGs) under alkaline stress. (**A**) Volcano plots illustrating the distribution of DEGs in the comparisons of TLD vs. LD (left) and TLD vs. TWL (right). Each dot represents a gene, with red and green dots indicating significantly upregulated and downregulated genes, respectively, based on thresholds of $|\log_2\text{FoldChange}| > 1$ and adjusted p-value < 0.05. These results highlight distinct transcriptional responses between control and stress conditions (TLD vs. LD), and between tolerant and sensitive genotypes under stress (TLD vs. TWL). (**B**) Hierarchical clustering heatmaps of DEGs across different conditions, indicating transcriptomic variation among the LD, TLD, WL, and TWL groups. (**C**) Venn diagram illustrating the overlap of DEGs across different comparisons (TLD vs. LD, TWL vs. WL, LD vs. WL, and TLD vs. TWL). A total of 829 genes were commonly differentially expressed across multiple comparisons. (For interpretation of the references to color in this figure legend, the reader is referred to the web version of this article.)

omes (KEGG) enrichment analyses were performed. GO enrichment analysis (Fig. 2A) revealed significant enrichment of genes related to oxidative stress response, hydrogen peroxide metabolism, and salt stress regulation, consistent with known stress adaptation mechanisms.

The GO term enrichment bar plots (Fig. 2B, **Fig. S1A**) illustrate distinct differences between the tolerant and sensitive varieties. In the TLD vs. TWL comparison, genes associated with antioxidant defense, ion transport, and membrane stability were significantly enriched, suggesting that Qijing 10 employs an active transcriptional strategy to mitigate alkali-induced stress. In contrast, genes involved in stress response signaling and secondary metabolite biosynthesis showed greater enrichment in TWL, potentially reflecting a compensatory response to alkali-induced damage. KEGG enrichment analysis (Fig. 2C, **Fig. S1B**) further highlighted key metabolic and signaling pathways involved in alkali stress adaptation. The fatty acid metabolism, plant hormone signal transduction, and flavonoid biosynthesis pathways were prominently enriched in the TLD vs. TWL group, consistent with the metabolomic findings that suggested lipid metabolism and antioxidant defense play crucial roles in alkali tolerance. The pathway enrichment scatter plots reveal that amino acid metabolism pathways, particularly those related to proline and glutamate metabolism, were more active in the tolerant variety, likely contributing to osmotic balance and redox homeostasis.

3.3. Transcription factor family distribution analysis of differentially expressed genes

Transcription factors (TFs) play a crucial role in modulating stress responses by regulating downstream gene expression [34,35]. To explore transcriptional regulatory mechanisms under alkali stress, we analyzed the distribution of differentially expressed TF families and their associated metabolic pathways.

KEGG classification analysis (Fig. 3A) showed that DEGs were predominantly enriched in pathways related to amino acid metabolism, carbohydrate metabolism, and plant hormone signal transduction. These pathways are central to stress adaptation, influencing osmotic regulation, energy metabolism, and signaling cascades. The involvement of butanoate metabolism and biosynthesis of secondary metabolites suggests that metabolic adjustments in response to alkali stress are at least partially transcriptionally regulated.

The pathway enrichment bubble plots (Fig. 3B**, Fig. S1C**) further highlight significant transcriptional regulation in key stress-related metabolic pathways. Notably, in the TLD vs. TWL comparison, genes involved in proline and glutamate metabolism, flavonoid biosynthesis, and fatty acid metabolism were significantly enriched, suggesting that alkali-tolerant varieties utilize a more refined transcriptional response to maintain cellular homeostasis.

Transcription factor family distribution analysis (Fig. 3C) revealed that WRKY, MYB, NAC, and bHLH families were among the most enriched TF groups. The WRKY family, known for its role in stress-responsive transcriptional regulation, was predominantly upregulated in the tolerant variety, suggesting its involvement in antioxidant defense and ion transport regulation. Similarly, the MYB and NAC families, which regulate flavonoid biosynthesis and secondary metabolite production, exhibited distinct expression patterns between TLD and TWL, reflecting divergent transcriptional responses to alkali stress.

Overall, these findings indicate that transcriptional regulation under alkali stress involves both metabolic reprogramming and stress signal transduction, with specific TF families coordinating adaptive responses in the tolerant variety. The observed transcriptional stability in Qijing 10 may be attributed to pre-existing regulatory mechanisms that facilitate a more controlled response to alkali-induced stress, in contrast to the extensive reprogramming observed in Tengxi 138.

A

GO Enrichment List of Differentially Expressed Genes

GO accession	Description	Term type	Over represented p-Value	Corrected p-Value
G0:0052736	beta-glucanase activity	Molecular function	1. 88e-03	1.00e+00
GO:0052861	glucan endo-1,3-beta-glucanase activity, C-3 substituted reducing group	Molecular function	1. 88e-03	1.00e+00
GO:0010310	regulation of hydrogen peroxide metabolic process	Biological process	5.21e-03	1.00e+00
GO:1902074	response to salt	Biological process	6.19e-03	1.00e+00
GO:0004351	glutamate decarboxylase activity	Molecular function	6.34e-03	1.00e+00
GO:1902882	regulation of response to oxidative stress	Biological process	6.55e-03	1.00e+00

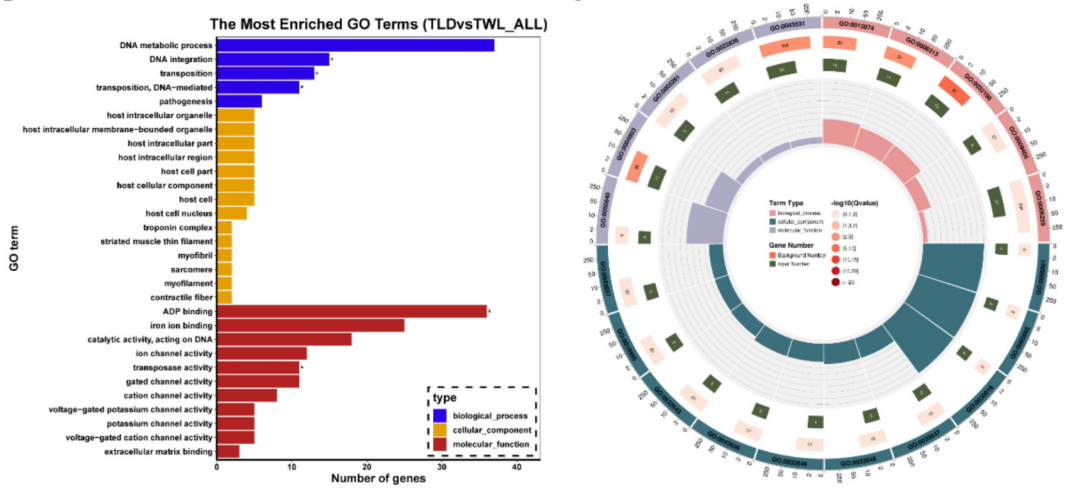

Fig. 2. Gene Ontology (GO) enrichment analysis of differentially expressed genes (DEGs). (**A**) Table presenting selected significantly enriched GO terms identified from DEGs, categorized into molecular function and biological process classifications, along with their associated overrepresentation *p*-values and corrected p-values. (**B**) Bar plot displaying the distribution of DEGs among the top enriched GO terms in the TLD vs. TWL comparison. GO terms are color-coded based on their classification into biological processes, molecular functions, and cellular components. (**C**) Circular visualization of GO enrichment results showing the gene distribution across different GO categories, with inner rings representing enrichment significance and outer labels indicating specific GO terms.

A

KEGG Enrichment List of Differentially Expressed Genes

kegg level1 term	kegg level2 term	kegg level3 term
Metabolism	Metabolism of other amino acids	Taurine and hypotaurine metabolism
Metabolism	Carbohydrate metabolism	Butanoate meta bolism
Metabolism	Meta bolism of other amino acids	beta-Alanine metabolism
Metabolism	Amino acid metabolism	Alanine, aspartate and glutamate metabolis
Environmental Information Processing	Signal transduction	Plant hormone signal transduction
Metabolism	Global and overview maps	Biosynthesis of secondary metabolites

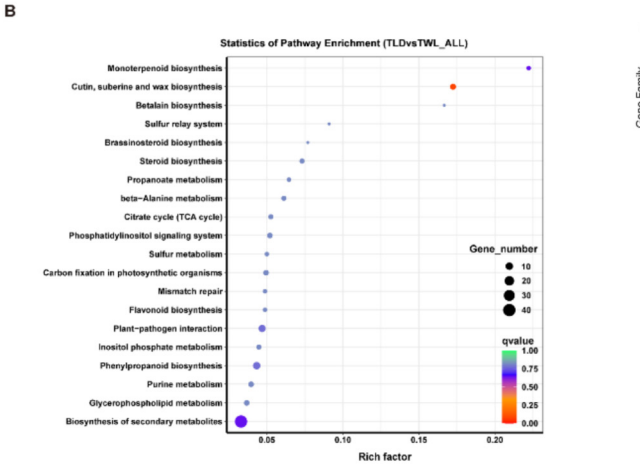

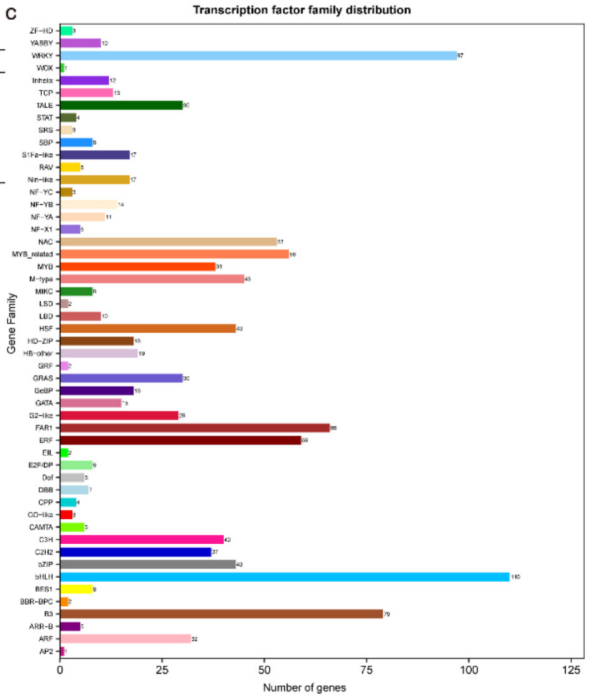

Fig. 3. KEGG enrichment analysis and transcription factor family distribution of differentially expressed genes (DEGs). (**A**) Summary table of KEGG pathway terms enriched among DEGs, organized into categories such as metabolism and signal transduction, with detailed classification into KEGG level 2 and level 3 terms. (**B**) Bubble plot showing significantly enriched KEGG pathways in the TLD vs. TWL comparison, with color indicating the adjusted *p*-value and bubble size representing the number of enriched genes. (**C**) Bar chart showing the classification of DEGs into transcription factor (TF) families. Each bar represents a TF family, with its length indicating the number of DEGs annotated to that family.

3.4. Metabolomic profiling reveals differential metabolic responses to alkali stress in rice

In this study, untargeted metabolomics analysis based on UHPLC-MS/MS was performed to investigate metabolic changes in the alkali-tolerant rice variety Qijing 10 (LD) and the alkali-sensitive variety Tengxi 138 (WL) before and after alkali stress treatment (TLD and TWL, respectively). A total of 1093 metabolites were detected. Principal component analysis (PCA), orthogonal partial least squares discriminant analysis (OPLS-DA), and hierarchical clustering heatmap analyses were applied to systematically evaluate metabolic variations across different samples, aiming to elucidate the metabolic basis of alkali tolerance in rice [36].

PCA revealed distinct metabolic profiles among the treatment groups. Along PC1 (28.4% variance explained) and PC2 (23.4% variance explained), the alkali-treated groups (TLD and TWL) exhibited clear separation from their respective controls (LD and WL), suggesting significant metabolic alterations induced by alkali stress. Additionally, QC samples clustered tightly, confirming the reliability and stability of the dataset. Notably, the metabolic profile of TLD was more similar to LD, whereas TWL exhibited a greater degree of metabolic perturbation compared to WL, indicating a stronger metabolic homeostasis regulation in the alkali-tolerant genotype (Fig. 4A). The hierarchical clustering heatmap further corroborated the PCA results, revealing distinct metabolic clustering patterns among samples. Biological replicates within the same treatment group exhibited high similarity, whereas significant differences were observed between alkali-treated and control groups. In particular, the metabolic profiles of TWL and WL differed markedly, suggesting that alkali stress induced more extensive metabolic reprogramming in the sensitive variety. Conversely, Qijing 10 retained metabolic characteristics similar to its control condition, indicating potential adaptive metabolic mechanisms that mitigate the impact of alkali stress (Fig. 4B). To further explore metabolic variations, pairwise OPLS-DA analyses were performed. The OPLS-DA model comparing LD and TLD demonstrated significant separation along the T-score (24.5%) and orthogonal T-score (32.5%) axes, indicating that alkali stress induced extensive metabolic remodeling in Qijing 10, possibly involving osmotic regulation, antioxidant metabolism, and energy metabolism. Similarly, the WL vs. TWL comparison exhibited pronounced separation along the T-score (24.7%) and orthogonal T-score (27.0%) axes, suggesting that the alkali-sensitive variety (Tengxi 138) experienced more severe metabolic perturbations under alkali stress. Furthermore, direct comparison between TLD and TWL revealed significant metabolic differences along the T-score (29.0%) and orthogonal T-score (31.3%) axes, highlighting distinct metabolic adaptation strategies between the tolerant and sensitive genotypes (Fig. 4C, **Fig. S2A**).

3.5. Identification and characterization of differential metabolites in alkali-tolerant and sensitive rice varieties

In this study, UHPLC-MS/MS-based untargeted metabolomics analysis was performed in combination with OPLS-DA and univariate statistical analysis to systematically investigate the metabolic adaptations of salt-alkali-tolerant and salt-alkali-sensitive rice varieties under alkaline stress. Key differential metabolites associated with alkaline stress response were identified based on the OPLS-DA model, with selection criteria including a variable importance in projection (VIP) score > 1, p-value < 0.05, and fold change >1.5 or <0.67. To ensure biological relevance, the analysis focused on two key comparisons: LD vs. TLD (metabolic changes in the salt-alkali-tolerant variety Qijing 10 before and after alkaline stress) and TLD vs. TWL (differences in metabolic adaptation between salt-alkali-tolerant and salt-alkali-sensitive varieties under alkaline stress), aiming to elucidate the core metabolic characteristics underlying salt-alkali tolerance. VIP score ranking

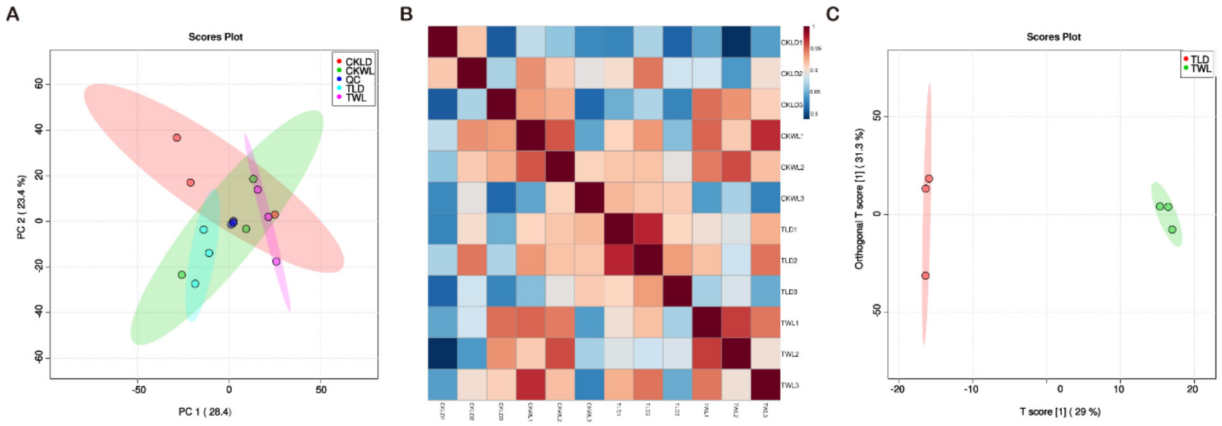

Fig. 4. Multivariate statistical analysis of metabolomic data under alkali stress. (**A**) Principal component analysis (PCA) score plot showing the distribution of samples across different experimental groups, with distinct clustering patterns indicating metabolic differences. (**B**) Correlation heatmap of metabolite profiles across all samples. The color scale represents Pearson correlation coefficients, indicating the similarity between individual samples based on their metabolite abundance profiles. (**C**) Orthogonal partial least squares discriminant analysis (OPLS-DA) score plot comparing TLD and TWL groups. The clear separation between groups suggests distinct metabolic responses to alkali stress in tolerant versus sensitive rice varieties. The X- and Y-axes represent the T-score and orthogonal T-score, respectively, summarizing between-group and within-group variation.

revealed key metabolites in LD vs. TLD, including maltotriose, 2,2-dichloro-1,1-ethanediol, and momordicoside I, which are primarily involved in carbohydrate metabolism, antioxidant defense, and osmotic regulation (**Fig. S2B**). The significant changes in these metabolites suggest that the salt-alkali-tolerant variety may enhance its ability to regulate osmotic balance and mitigate reactive oxygen species (ROS) accumulation under alkaline stress. In TLD vs. TWL, the most highly ranked VIP metabolites included alangicine, folinic acid, diosmin, and phloroglucinol carboxylic acid, indicating distinct metabolic differences in alkaline stress adaptation between the tolerant and sensitive varieties (Fig. 5A).

Volcano plot analysis further highlighted the overall impact of alkaline stress on metabolite profiles. In LD vs. TLD, a total of 65 significantly differentially expressed metabolites were identified, with 27 upregulated and 38 downregulated (**Fig. S2C**). These findings suggest that the salt-alkali-tolerant variety undergoes extensive metabolic remodeling to maintain homeostasis and enhance adaptation to stress. In contrast, TLD vs. TWL revealed 102 differentially expressed metabolites, with 28 upregulated and 74 downregulated (Fig. 5B), indicating that the salt-alkali-sensitive variety exhibits a greater degree of metabolic imbalance under alkaline conditions. Fold change bar plots further illustrated the specific trends in metabolite changes. In LD vs. TLD, metabolites such as D-erythro-MAPP, O-desmethylquinidine glucuronide, and 2,2-dichloro-1,1-ethanediol were significantly upregulated (**Fig. S2D**). In TLD vs. TWL, metabolites including penicillin G, catalposide, and alangicine were upregulated in the salt-alkali-tolerant variety, while diosmin, neocustoside C, and fumonisin FP1 were significantly downregulated in the salt-alkali-sensitive variety (Fig. 5C). These metabolic alterations may be closely associated with the physiological mechanisms underlying salt-alkali tolerance. To further investigate the dynamic patterns of metabolite changes across different experimental groups, K-means clustering analysis was performed, classifying differential metabolites into four major clusters (Fig. 5D). One cluster (Cluster 2) exhibited significant upregulation following alkaline stress, suggesting its potential role in stress adaptation, whereas another cluster (Cluster 1) showed a decline after alkaline stress, which was partially recovered in the salt-alkali-sensitive variety, possibly reflecting a compensatory metabolic response. Additionally, hierarchical clustering analysis revealed distinct metabolic patterns among the experimental groups. The metabolic differences between LD and TLD suggest that the salt-alkali-tolerant variety undergoes substantial metabolic remodeling in response to alkaline stress, while the pronounced differences between TLD and TWL further emphasize the critical influence of genetic background on metabolic adaptation.

Overall, our findings suggest that the salt-alkali-tolerant variety enhances its alkaline stress tolerance through regulation of carbohydrate metabolism, strengthening of antioxidant defenses, and modulation of osmoprotectant accumulation, whereas the salt-alkali-sensitive variety exhibits greater metabolic fluctuations under similar stress conditions.

3.6. Metabolic pathway enrichment analysis of differential metabolites under alkali stress

To further investigate the metabolic changes and potential biological significance of different alkali-tolerant rice varieties under alkaline stress conditions, we performed metabolic pathway enrichment analysis on the identified differential metabolites and visualized key metabolic pathways. Metabolite clustering analysis (Fig. 6A) revealed distinct overall distribution patterns of metabolites among different treatment groups, with significant metabolic profile changes observed particularly in the alkali-tolerant variety (TLD) and the sensitive variety (TWL) after alkali treatment. This suggests that alkaline stress induces varying degrees of metabolic reprogramming, necessitating further pathway enrichment analysis to elucidate the functional implications of these changes.

KEGG pathway enrichment analysis indicated significant alterations in multiple metabolic pathways under alkaline stress conditions. In the LD vs. TLD comparison (**Fig. S3A**), the most enriched pathways were primarily associated with fatty acid degradation, glutathione metabolism, and fatty acid elongation, which may contribute to the alkali-tolerant variety's adaptation through enhanced lipid metabolism and antioxidant defense mechanisms. In contrast, the TLD vs. TWL comparison (Fig. 6B) revealed significant enrichment of metabolic pathways related to membrane stability and stress responses, such as alpha-linolenic acid metabolism, anthocyanin biosynthesis, and carotenoid biosynthesis, suggesting that alkali-tolerant varieties may improve tolerance by modulating membrane lipid composition and antioxidant metabolism. Further pathway classification analysis demonstrated that most differential metabolites were enriched in metabolism-related pathways, particularly lipid metabolism, amino acid metabolism, and secondary metabolic pathways. In the LD vs. TLD group

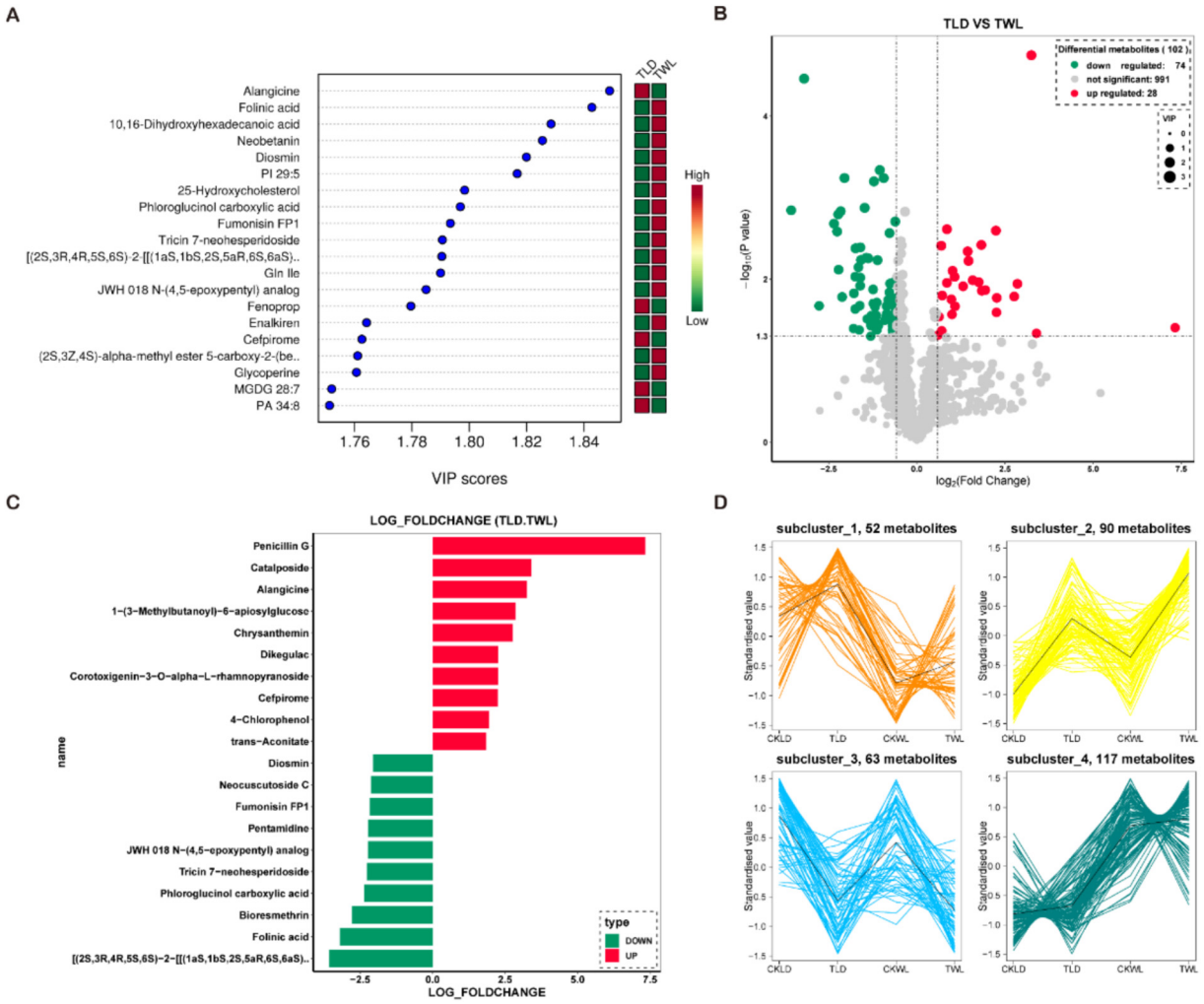

Fig. 5. Identification of key differential metabolites between TLD and TWL under alkali stress. (**A**) Variable importance in projection (VIP) score plot from the OPLS-DA model, showing the top metabolites contributing to the discrimination between TLD and TWL. Heatmap on the right indicates the relative abundance of selected metabolites across samples. (**B**) Volcano plot illustrating the distribution of DAMs based on fold change (log_2 scale) and statistical significance ($-log_{10}P$). Red and green dots represent upregulated and downregulated metabolites, respectively, based on VIP > 1 and $p < 0.05$. (**C**) Bar chart showing log_2 fold changes of selected representative DAMs in TLD versus TWL, providing an overview of the magnitude and direction of metabolite changes. (**D**) K-means clustering analysis grouping DAMs into four subclusters based on abundance patterns across all experimental groups (CKLD, CKWL, TLD, and TWL). Each cluster displays distinct expression trends, reflecting potential functional categorization or regulation under different conditions. (For interpretation of the references to color in this figure legend, the reader is referred to the web version of this article.)

(**Fig. S3B**), metabolites were primarily concentrated in fatty acid degradation, flavonoid biosynthesis, and terpenoid backbone biosynthesis, whereas the TLD vs. TWL group (Fig. 6C) exhibited greater involvement in fatty acid biosynthesis and arginine and proline metabolism. These pathway alterations likely play crucial roles in determining alkali stress tolerance among different rice varieties. Moreover, KEGG classification analysis further elucidated the distribution of differentially expressed metabolites across metabolic pathways. The classification results showed that the majority of significantly altered metabolites were involved in primary metabolism, particularly fatty acid metabolism, secondary metabolite biosynthesis, and cellular environmental responses. Notably, the LD vs. TLD group (**Fig. S3C**) exhibited enrichment in lipid and flavonoid metabolism, whereas the TLD vs. TWL group (Fig. 6D) displayed distinct metabolic pathway involvement, including responses to oxidative stress and membrane structural modifications. These findings suggest that the alkali-tolerant variety may possess enhanced metabolic plasticity to mitigate the detrimental effects of alkaline stress.

In all, this study utilized KEGG pathway enrichment and classification analyses to reveal the key metabolic adaptation mechanisms of alkali-tolerant rice varieties under alkaline stress. The significant changes observed in major metabolic pathways, such as fatty acid metabolism, glutathione metabolism, and flavonoid biosynthesis, provide critical insights for further elucidating the physiological regulatory mechanisms underlying alkali tolerance in rice.

4. Discussion

Alkaline stress is a major abiotic factor that affects crop growth and productivity by disrupting cellular homeostasis, nutrient uptake, and metabolic stability. Understanding how different rice varieties respond to such stress at both the transcriptomic and metabolomic levels is crucial for identifying adaptive mechanisms and potential targets for breeding stress-tolerant cultivars [37,38,39]. In this study, we performed a comprehensive transcriptomic and metabolomic analysis to compare the responses of an

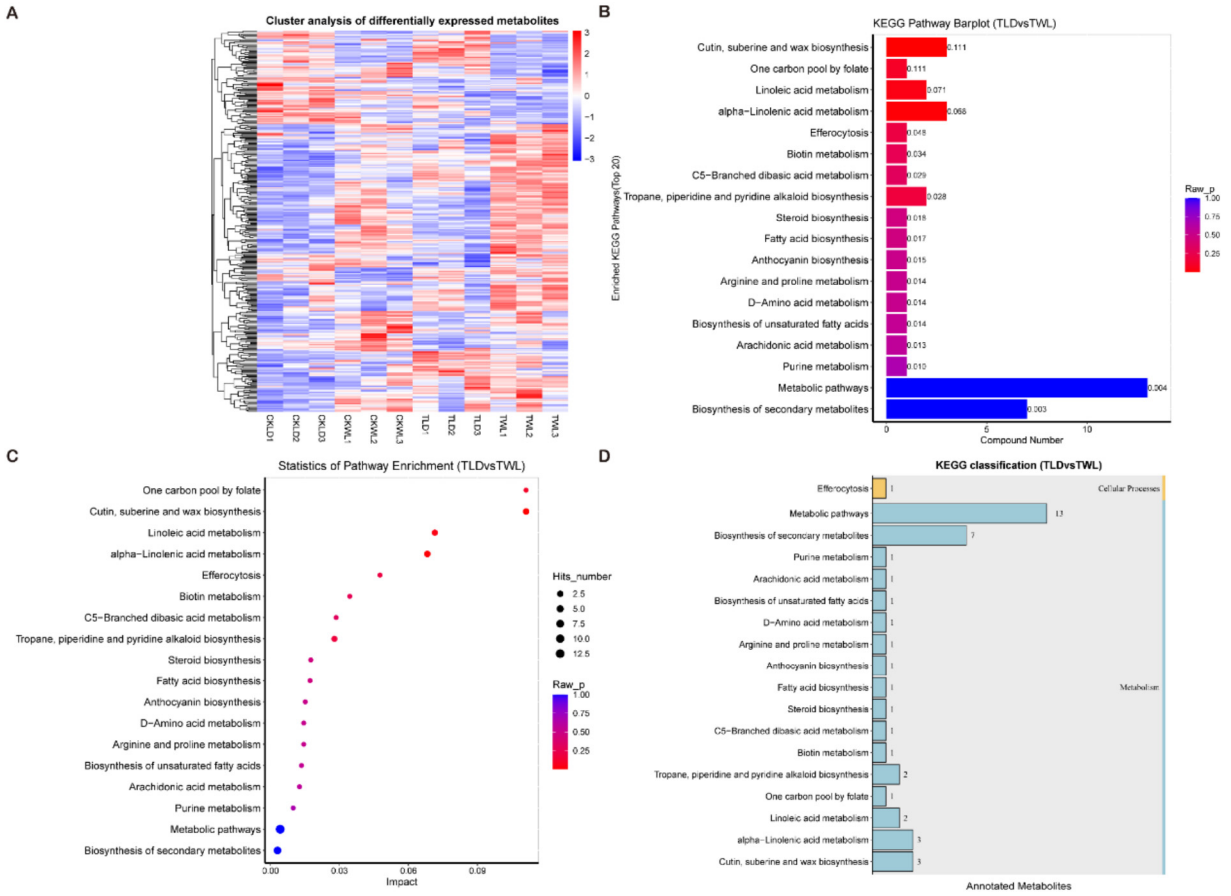

Fig. 6. Metabolomic analysis of differentially accumulated metabolites (DAMs) and pathway enrichment in TLD vs. TWL. (**A**) Heatmap of differentially accumulated metabolites across all sample groups (CKLD, CKWL, TLD, TWL), showing hierarchical clustering based on abundance patterns. (**B**) KEGG pathway bar plot presenting the number of annotated DAMs involved in each significantly enriched pathway. Pathways are arranged by enrichment significance, with color scale indicating the corresponding $-\log_{10}(p\text{-value})$. (**C**) Bubble plot showing KEGG pathway enrichment analysis, with impact scores and statistical significance (p-value). (**D**) KEGG classification of annotated metabolites, categorizing them into primary metabolic and cellular processes.

alkali-tolerant rice variety (Qijing 10) and an alkali-sensitive variety (Tengxi 138) under control and alkali-stressed conditions, revealing fundamentally distinct adaptation strategies. While Qijing 10 maintains metabolic homeostasis through coordinated regulation, Tengxi 138 exhibits fragmented responses characterized by transcriptional hyperactivity and metabolic instability. This dichotomy mirrors observations in salt-sensitive versus salt-tolerant crops, suggesting conserved principles of stress resilience across abiotic challenges.

One of the most significant findings of this study is that the alkali-tolerant variety employs well-regulated metabolic strategies to cope with stress. Metabolomic analysis showed that lipid metabolism, oxidative stress defense, and osmotic regulation play key roles in alkali tolerance. Specifically, the KEGG enrichment analysis revealed that fatty acid degradation and biosynthesis pathways were more active in the tolerant variety under stress. Fatty acid metabolism is essential for maintaining membrane integrity and fluidity under abiotic stress [40]. Recent studies further demonstrate that polyamine-modified lipids (e.g., phenolamides) can stabilize membranes under salinity by interacting with phospholipids, as shown in tomato [41]. This aligns with our finding that lipid remodeling in Qijing 10 enhances cellular protection, possibly through similar mechanisms. Supporting this, transcriptomic analysis identified upregulation of genes involved in lipid metabolism, including ACX and KCS family genes, which contribute to fatty acid β-oxidation and elongation [42]. These findings suggest that lipid metabolism is a critical factor in alkali stress adaptation. Another key adaptive mechanism observed in the tolerant variety was enhanced antioxidant defense. The GO and KEGG analyses revealed significant enrichment in glutathione metabolism, flavonoid biosynthesis, and hydrogen peroxide decomposition pathways. Increased expression of genes encoding antioxidant enzymes, such as glutathione peroxidase and ascorbate peroxidase, suggests that Qijing 10 can efficiently neutralize ROS generated under alkali stress. This aligns with previous studies showing that antioxidant systems play a crucial role in stress tolerance by mitigating oxidative damage. Additionally, flavonoid biosynthesis, regulated by MYB transcription factors, was more active in the tolerant variety, suggesting a role in ROS scavenging and secondary metabolite-mediated defense [43,44,45,46]. Osmotic regulation through amino acid metabolism was another prominent feature of alkali tolerance in Qijing 10. The transcriptomic and metabolomic results showed significant enrichment in proline, glutamate, and arginine metabolism under alkali stress. Proline accumulation has been widely reported as a protective strategy against osmotic stress, serving as an osmoprotectant and stabilizing cellular structures [47,48]. The upregulation of P5CS and OAT genes, which regulate proline biosynthesis, further supports the role of osmotic regulation in stress adaptation.

In contrast to the well-coordinated metabolic adjustments observed in Qijing 10, the alkali-sensitive variety (Tengxi 138) exhibited signs of metabolic-transcriptional decoupling under stress. The KEGG enrichment analysis indicated that sugar metabolism, amino acid metabolism, and secondary metabolite biosynthe-

sis pathways were highly affected. However, metabolite accumulation patterns were inconsistent, suggesting that the sensitive variety undergoes a more disruptive metabolic response rather than a regulated adaptation. Transcriptomic analysis of TWL vs. WL revealed the upregulation of several stress-responsive transcription factors, including NAC and bZIP, which are known to be involved in abiotic stress responses [49,50]. However, unlike in Qijing 10, these transcriptional changes did not correlate with a stable metabolic adjustment, implying that Tengxi 138 relies on rapid gene expression shifts rather than sustained metabolic regulation. This aligns with studies suggesting that stress-sensitive plants often activate a broad, but less efficient, transcriptional response to environmental challenges [51].

A key advantage of this study is the integration of transcriptomic and metabolomic data. This approach mirrors advances in stress metabolomics, where gene clusters (e.g., polyamine transporters and modifying enzymes) are increasingly linked to metabolite-mediated tolerance [41]. Our identification of co-regulated lipid/antioxidant pathways in Qijing 10 extends this framework to alkali stress, highlighting conserved metabolic modules across stress types, which allows us to establish direct links between gene expression changes and metabolic adaptations [52,53,54]. Pathway enrichment analysis demonstrated that transcriptional regulation directly influenced metabolic stability in the tolerant variety. For example, in the fatty acid metabolism pathway, transcriptomic data showed upregulation of ACX and KCS genes, which corresponded to an increased abundance of lipid-related metabolites in the metabolomic data. Similarly, glutathione metabolism and flavonoid biosynthesis were upregulated at both the transcriptional and metabolic levels, reinforcing the role of antioxidant defense in alkali tolerance. In contrast, while the sensitive variety displayed increased expression of stress-responsive genes, these transcriptional changes did not lead to a stable metabolic adaptation. For instance, secondary metabolite biosynthesis genes were upregulated, but the metabolomic data indicated fluctuations in metabolite accumulation, suggesting inefficient metabolic control. This highlights a fundamental difference between tolerant and sensitive varieties: the tolerant variety exhibits a more synchronized transcriptomic and metabolomic response, while the sensitive variety relies on transcriptional activation without sustained metabolic reinforcement [55,56].

This study provides valuable insights into the molecular basis of alkali tolerance in rice and offers potential targets for breeding stress-resilient cultivars. The identification of key metabolic pathways, such as lipid metabolism, antioxidant defense, and osmotic regulation, provides a foundation for future functional studies aimed at improving stress tolerance. Additionally, the discovery that WRKY, MYB, and NAC transcription factors regulate stress-related metabolic pathways highlights the potential for targeted genetic modifications to enhance alkali tolerance.

While our untargeted metabolomics approach provides broad coverage of metabolic changes, it carries inherent limitations in distinguishing endogenous metabolites from environmental contaminants. Compounds such as triclosan and digitoxin, though detected, were excluded from biological interpretation after consulting rice-specific metabolite databases (e.g., RiceCyc) and confirming their absence in prior literature. Future targeted metabolomics focusing on stress-related metabolite classes (e.g., polyamines, phenolic compounds) could provide more definitive quantification of these functional components.

CRediT authorship contribution statement

Jiangxu Wang: Project administration, Conceptualization, Funding acquisition, Writing – review & editing. **Chuang Lang:** Data curation, Investigation, Methodology. **Yang Ren:** Formal analysis. **Junxiang Guo:** Data curation. **Wendong Ma:** Resources, Software. **Qing Liu:** Writing – original draft. **Lei Lei:** Data curation, Resources. **Shichen Sun:** Writing – review & editing, Funding acquisition, Conceptualization, Project administration.

Financial support

This work was supported by the following funding sources: the Provincial Scientific Research Institutions Research Fund of Heilongjiang Province (CZKYF2025-1-B010) for "Application of Grain Shape Mutagenesis Mutants in Cold-Region Rice Breeding"; the Major Project of "Agricultural Science and Technology Innovation Leap Project" of Heilongjiang Academy of Agricultural Sciences (CX23ZD02) for "Breeding, Promotion, and Industrial Development of Medium-Late Maturing, High-Quality, High-Yield, and Broad-Adaptability Rice Varieties"; the Natural Science Foundation of Heilongjiang Province (JQ2022C03); the National Modern Agricultural Industry Technology System Special Funds (CARS-01-55); and the National Key Research and Development Program of China (2024YFD1201002).

Declaration of competing interest

The authors declare that they have no known competing financial interests or personal relationships that could have appeared to influence the work reported in this paper.

Supplementary material

https://doi.org/10.1016/j.ejbt.2025.07.002.

Data availability

No data was used for the research described in the article.

References

[1] Zhang H, Yu F, Xie P, et al. A Gγ protein regulates alkaline sensitivity in crops. Science 2023;379(6638):eade8416. https://doi.org/10.1126/science.ade8416. PMid: 36952416.
[2] Kaiwen G, Zisong X, Yuze H, et al. Effects of salt concentration, pH, and their interaction on plant growth, nutrient uptake, and photochemistry of alfalfa (*Medicago sativa*) leaves. Plant Signal Behav 2020;15(12):1832373. https://doi.org/10.1080/15592324.2020.1832373. PMid: 33073686.
[3] Zhang H, Liu XL, Zhang RX, et al. Root damage under alkaline stress is associated with reactive oxygen species accumulation in rice (*Oryza sativa* L.). Front Plant Sci 2017;8:1580. https://doi.org/10.3389/fpls.2017.01580. PMid: 28943882.
[4] Fang S, Hou X, Liang X. Response mechanisms of plants under saline-alkali stress. Front Plant Sci 2021;12:667458. https://doi.org/10.3389/fpls.2021.667458. PMid: 34149764.
[5] Yu J, Li Y, Qin Z, et al. Plant chloroplast stress response: Insights from thiol redox proteomics. Antioxid Redox Signal 2020;33(1):35–57. https://doi.org/10.1089/ars.2019.7823. PMid: 31989831.
[6] Cao Y, Song H, Zhang L. New insight into plant saline-alkali tolerance mechanisms and application to breeding. Int J Mol Sci 2022;23(24):16048. https://doi.org/10.3390/ijms232416048. PMid: 36555693.
[7] Fan C. Genetic mechanisms of salt stress responses in halophytes. Plant Signal Behav 2020;15(1):1704528. https://doi.org/10.1080/15592324.2019.1704528. PMid: 31868075.
[8] Yu X, Liu Z, Sun X. Single-cell and spatial multi-omics in the plant sciences: Technical advances, applications, and perspectives. Plant Commun 2023;4(3):100508. https://doi.org/10.1016/j.xplc.2022.100508. PMid: 36540021.
[9] Feng Z, Ding C, Li W, et al. Applications of metabolomics in the research of soybean plant under abiotic stress. Food Chem 2020;310:125914. https://doi.org/10.1016/j.foodchem.2019.125914. PMid: 31835223.
[10] Seyfferth C, Renema J, Wendrich JR, et al. Advances and opportunities in single-cell transcriptomics for plant research. Annu Rev Plant Biol 2021;72:847–66. https://doi.org/10.1146/annurev-arplant-081720-010120. PMid: 33730513.

[11] Allwood JW, Williams A, Uthe H, et al. Unravelling plant responses to stress-the importance of targeted and untargeted metabolomics. Metabolites 2021;11(8):558. https://doi.org/10.3390/metabo11080558. PMid: 34436499.
[12] Yang Y, Guo Y. Elucidating the molecular mechanisms mediating plant salt-stress responses. New Phytol 2018;217(2):523–39. https://doi.org/10.1111/nph.14920. PMid: 29205383.
[13] Jorge TF, Rodrigues JA, Caldana C, et al. Mass spectrometry-based plant metabolomics: Metabolite responses to abiotic stress. Mass Spectrom Rev 2016;35(5):620–49. https://doi.org/10.1002/mas.21449. PMid: 25589422.
[14] Yan J, Wang X. Machine learning bridges omics sciences and plant breeding. Trends Plant Sci 2023;28(2):199–210. https://doi.org/10.1016/j.tplants.2022.08.018. PMid: 36153276.
[15] Zhao C, Zhang H, Song C, et al. Mechanisms of plant responses and adaptation to soil salinity. Innovation 2020;1(1):100017. https://doi.org/10.1016/j.xinn.2020.100017. PMid: 34557705.
[16] Zhu JK. Abiotic stress signaling and responses in plants. Cell 2016;167(2):313–24. https://doi.org/10.1016/j.cell.2016.08.029. PMid: 27716505.
[17] Zhang H, Zhu J, Gong Z, et al. Abiotic stress responses in plants. Nat Rev Genet 2022;23(2):104–19. https://doi.org/10.1038/s41576-021-00413-0. PMid: 34561623.
[18] Danquah A, de Zelicourt A, Colcombet J, et al. The role of ABA and MAPK signaling pathways in plant abiotic stress responses. Biotechnol Adv 2014;32(1):40–52. https://doi.org/10.1016/j.biotechadv.2013.09.006. PMid: 24091291.
[19] Xu X, Zhang J, Yan B, et al. The adjustment of membrane lipid metabolism pathways in maize roots under saline-alkaline stress. Front Plant Sci 2021;12:635327. https://doi.org/10.3389/fpls.2021.635327. PMid: 33790924.
[20] Qian G, Wang M, Wang X, et al. Integrated transcriptome and metabolome analysis of rice leaves response to high saline-alkali stress. Int J Mol Sci 2023;24(4):4062. https://doi.org/10.3390/ijms24044062. PMid: 36835473.
[21] Sagervanshi A, Geilfus CM, Kaiser H, et al. Alkali salt stress causes fast leaf apoplastic alkalinization together with shifts in ion and metabolite composition and transcription of key genes during the early adaptive response of *Vicia faba* L. Plant Sci 2022;319:111253. https://doi.org/10.1016/j.plantsci.2022.111253. PMid: 35487662.
[22] Ma S, Lv L, Meng C, et al. Integrative analysis of the metabolome and transcriptome of *Sorghum bicolor* reveals dynamic changes in flavonoids accumulation under saline-alkali stress. J Agric Food Chem 2020;68(50):14781–9. https://doi.org/10.1021/acs.jafc.0c06249. PMid: 33274637.
[23] Zhang Z, Zhang F, Deng Y, et al. Integrated metabolomics and transcriptomics analyses reveal the metabolic differences and molecular basis of nutritional quality in landraces and cultivated rice. Metabolites 2022;12(5):384. https://doi.org/10.3390/metabo12050384. PMid: 35629888.
[24] Hara Y, Tatsumi K, Yoshida M, et al. Optimizing and benchmarking *de novo* transcriptome sequencing: From library preparation to assembly evaluation. BMC Genomics 2015;16:977. https://doi.org/10.1186/s12864-015-2007-1. PMid: 26581708.
[25] Hrdlickova R, Toloue M, Tian B. RNA-Seq methods for transcriptome analysis. Wiley Interdiscip Rev RNA 2017;8(1):e1364. https://doi.org/10.1002/wrna.1364. PMid: 27198714.
[26] Wang Z, Gerstein M, Snyder M. RNA-Seq: A revolutionary tool for transcriptomics. Nat Rev Genet 2009;10(1):57–63. https://doi.org/10.1038/nrg2484. PMid: 19015660.
[27] Trapnell C, Roberts A, Goff L, et al. Differential gene and transcript expression analysis of RNA-seq experiments with TopHat and Cufflinks. Nat Protoc 2012;7(3):562–78. https://doi.org/10.1038/nprot.2012.016. PMid: 22383036.
[28] Marquez Y, Brown JW, Simpson C, et al. Transcriptome survey reveals increased complexity of the alternative splicing landscape in *Arabidopsis*. Genome Res 2012;22(6):1184–95. https://doi.org/10.1101/gr.134106.111. PMid: 22391557.
[29] Volpi N, Galeotti F, Gatto F. High-throughput glycosaminoglycan extraction and UHPLC-MS/MS quantification in human biofluids. Nat Protoc 2024;20:843–60. https://doi.org/10.1038/s41596-024-01078-9. PMid: 39543382.
[30] Han K, Hua J, Zhang Q, et al. Multi-residue analysis of fipronil and its metabolites in eggs by SinChERS-Based UHPLC-MS/MS. Food Sci Anim Resour 2021;41(1):59–70. https://doi.org/10.5851/kosfa.2020.e76. PMid: 33506217.
[31] Chong J, Xia J. MetaboAnalystR: An R package for flexible and reproducible analysis of metabolomics data. Bioinformatics 2018;34(24):4313–4. https://doi.org/10.1093/bioinformatics/bty528. PMid: 29955821.
[32] Tautenhahn R, Cho K, Uritboonthai W, et al. An accelerated workflow for untargeted metabolomics using the METLIN database. Nat Biotechnol 2012;30(9):826–8. https://doi.org/10.1038/nbt.2348. PMid: 22965049.
[33] Boccard J, Rutledge DN. A consensus orthogonal partial least squares discriminant analysis (OPLS-DA) strategy for multiblock Omics data fusion. Anal Chim Acta 2013;769:30–9. https://doi.org/10.1016/j.aca.2013.01.022. PMid: 23498118.
[34] Huang Y, Sun Z, Zhou X. WRKY Transcription factors in response to metal stress in plants: A review. Int J Mol Sci 2024;25(20):10952. https://doi.org/10.3390/ijms252010952. PMid: 39456735.
[35] Li S, Han X, Lu Z, et al. MAPK Cascades and transcriptional factors: Regulation of heavy metal tolerance in plants. Int J Mol Sci 2022;23(8):4463. https://doi.org/10.3390/ijms23084463. PMid: 35457281.
[36] Maritha V, Harlina PW, Musfiroh I, et al. The application of chemometrics in metabolomic and lipidomic analysis data presentation for halal authentication of meat products. Molecules 2022;27(21):7571. https://doi.org/10.3390/molecules27217571. PMid: 36364396.
[37] Zhou Z, Liu J, Meng W, et al. Integrated analysis of transcriptome and metabolome reveals molecular mechanisms of rice with different salinity tolerances. Plants 2023;12(19):3359. https://doi.org/10.3390/plants12193359. PMid: 37836098.
[38] Wang J, Yan D, Liu R, et al. The physiological and molecular mechanisms of exogenous melatonin promote the seed germination of Maize (*Zea mays* L.) under salt stress. Plants 2024;13(15):2142. https://doi.org/10.3390/plants13152142. PMid: 39124260.
[39] Gechev TS, Dinakar C, Benina M, et al. Molecular mechanisms of desiccation tolerance in resurrection plants. Cell Mol Life Sci 2012;69(19):3175–86. https://doi.org/10.1007/s00018-012-1088-0. PMid: 22833170.
[40] Liu P, Wang Y, Yang G, et al. The role of short-chain fatty acids in intestinal barrier function, inflammation, oxidative stress, and colonic carcinogenesis. Pharmacol Res 2021;165:105420. https://doi.org/10.1016/j.phrs.2021.105420. PMid: 33434620.
[41] Yang J, Zhang Z, Li X, et al. A gene cluster for polyamine transport and modification improves salt tolerance in tomato. Plant J 2024;120(5):1706–23. https://doi.org/10.1111/tpj.17074. PMid: 39401077.
[42] Rizwan HM, Shaozhong F, Li X, et al. Genome-wide identification and expression profiling of KCS gene family in passion fruit (*Passiflora edulis*) under *Fusarium kyushuense* and drought stress conditions. Front Plant Sci 2022;13:872263. https://doi.org/10.3389/fpls.2022.872263. PMid: 35548275.
[43] Manna M, Thakur T, Chirom O, et al. Transcription factors as key molecular target to strengthen the drought stress tolerance in plants. Physiol Plant 2021;172(2):847–68. https://doi.org/10.1111/ppl.13268. PMid: 33180329.
[44] Ng DW, Abeysinghe JK, Kamali M. Regulating the regulators: The control of transcription factors in plant defense signaling. Int J Mol Sci 2018;19(12):3737. https://doi.org/10.3390/ijms19123737. PMid: 30477211.
[45] Ikram M, Batool M, Ullah M, et al. Molecular alchemy: Converting stress into resilience via secondary metabolites and calcium signaling in rice. Rice 2025;18(1):32. https://doi.org/10.1186/s12284-025-00783-7. PMid: 40325258.
[46] Nie S, Huang W, He C, et al. Transcription factor OsMYB2 triggers amino acid transporter *OsANT1* expression to regulate rice growth and salt tolerance. Plant Physiol 2025;197(2):kiae559. https://doi.org/10.1093/plphys/kiae559. PMid: 39425973.
[47] Kavi Kishor PB, Sreenivasulu N. Is proline accumulation *per se* correlated with stress tolerance or is proline homeostasis a more critical issue? Plant Cell Environ 2014;37(2):300–11. https://doi.org/10.1111/pce.12157. PMid: 23790054.
[48] Mattioli R, Costantino P, Trovato M. Proline accumulation in plants: Not only stress. Plant Signal Behav 2009;4(11):1016–8. https://doi.org/10.4161/psb.4.11.9797. PMid: 20009553.
[49] Seo PJ, Kim SG, Park CM. Membrane-bound transcription factors in plants. Trends Plant Sci 2008;13(10):550–6. https://doi.org/10.1016/j.tplants.2008.06.008. PMid: 18722803.
[50] Kumar D, Kirti PB. The genus *Arachis*: An excellent resource for studies on differential gene expression for stress tolerance. Front Plant Sci 2023;14:1275854. https://doi.org/10.3389/fpls.2023.1275854. PMid: 38023864.
[51] Rosenkranz RRE, Ullrich S, Löchli K, et al. Relevance and regulation of alternative splicing in plant heat stress response: Current understanding and future directions. Front Plant Sci 2022;13:911277. https://doi.org/10.3389/fpls.2022.911277. PMid: 35812973.
[52] Shi S, Zha W, Yu X, et al. Integrated transcriptomics and metabolomics analysis provide insight into the resistance response of rice against brown planthopper. Front Plant Sci 2023;14:1213257. https://doi.org/10.3389/fpls.2023.1213257. PMid: 37426975.
[53] Zhang Q, Li T, Gao M, et al. Transcriptome and metabolome profiling reveal the resistance mechanisms of rice against brown planthopper. Int J Mol Sci 2022;23(8):4083. https://doi.org/10.3390/ijms23084083. PMid: 35456901.
[54] Liu L, Li K, Zhou X, et al. Integrative analysis of metabolome and transcriptome reveals the role of strigolactones in wounding-induced rice metabolic re-programming. Metabolites 2022;12(9):789. https://doi.org/10.3390/metabo12090789. PMid: 36144193.
[55] Molisso D, Coppola M, Buonanno M, et al. Tomato prosystemin is much more than a simple systemin precursor. Biology 2022;11(1):124. https://doi.org/10.3390/biology11010124. PMid: 35053122.
[56] Li C, Jia Y, Zhou R, et al. GWAS and RNA-seq analysis uncover candidate genes associated with alkaline stress tolerance in maize (*Zea mays* L.) seedlings. Front Plant Sci 2022;13. https://doi.org/10.3389/fpls.2022.963874. PMid: 35923879.